

# An attempt to establish a statistical model of the day-to-day variability of the $N_mF2$ and $h_mF2$ parameters computed from IRI

Claudio Brunini<sup>a,\*</sup>, Francisco Azpilicueta<sup>a</sup>, Diego Janches<sup>b</sup>

<sup>a</sup> GESA, Facultad de Ciencias Astronómicas y Geofísicas, Universidad Nacional de La Plata, CONICET, Paseo del Bosque s/n, La Plata 1900, Argentina

<sup>b</sup> Goddard Space Flight Center, NASA, Greenbelt, MD 20771, USA

Received 28 December 2013; received in revised form 18 July 2014; accepted 22 July 2014

Available online 30 July 2014

## Abstract

In this work we explore the possibility of using COSMIC/FORMOSAT-3 radio occultation profiles (ROP) to establish a statistical model of the deviations that can be expected between the monthly median values of  $N_mF2$  and  $h_mF2$  computed with the International Reference Ionosphere (IRI) and the actual values of these parameters. The actual values are retrieved from the ROP after an interactively re-weighted Least Square fit that, complemented with a statistical test, allows filtering of unreliable data and estimating the errors of the retrieved values. The differences between the retrieved values and the monthly median values computed from IRI are interpreted as the superposition of a systematic bias (attributed to both, IRI and ROP), random errors in ROP, and the day-to-day variability, which is unaccounted for by IRI. This variability is described with a five-dimensional function that depends on: the month, the solar activity, the geomagnetic conditions, the modip latitude, and the local time. Empirical values of this function are estimated in the form of regular grids.

Since this research is restricted to low solar activity and quiet geomagnetic conditions, the grid is reduced from five to three dimensions: month, local time, and modip (modified dip latitude). We found that the standard deviation of the day-to-day variability varies according to (in percent of the monthly median value computed with IRI): (i)  $N_mF2$  at noontime:  $\pm 10\%$  to  $\pm 30\%$  with maxima over the northern and southern peaks of the Equatorial Anomaly; (ii)  $N_mF2$  at midnight:  $\pm 20\%$  to  $\pm 45\%$ , with the greatest values in the equatorial region during the months of May and September; (iii)  $h_mF2$  at noontime:  $\pm 2\%$  to  $\pm 10\%$  with minima over the modip equator; and (iv)  $h_mF2$  at midnight:  $\pm 3\%$  to  $\pm 11\%$  with the greatest values in the equatorial region from January to May and from September to January.

© 2014 COSPAR. Published by Elsevier Ltd. All rights reserved.

**Keywords:** Ionosphere; IRI;  $N_mF2$  and  $h_mF2$  variability

## 1. Introduction

This work is intended as a contribution toward developing a statistical model of the deviations that can be expected between the ionospheric electron density,  $N_mF2$ , and height,  $h_mF2$ , of the  $F2$  peak, computed with the International Reference Ionosphere (IRI; Bilitza et al., 2011),

and the actual values of these parameters. The procedure used to establish the model relies upon comparing the IRI parameters to the ones retrieved from the radio-occultation profiles (ROP) produced by the COSMIC/FORMOSAT-3 (C/F-3) mission (Anthes et al., 2008).

The primary parameters provided by IRI are the monthly median values of the critical frequency,  $f_oF2$ , and propagation factor,  $M_{3000}F2$ , of the  $F2$  peak. The computation technique implemented in IRI is based on the pioneering work of Jones and Gallet (1962) (further refined by Jones and Gallet (1965) and Jones and Obitts (1970)),

\* Corresponding author. Tel.: +54 221 4236593x154; fax: +54 221 4236591.

E-mail address: [claudiobrunini@yahoo.com](mailto:claudiobrunini@yahoo.com) (C. Brunini).

which, in the present work, is used in connection with the ITU-R coefficients (Radio Communication Sector of the International Telecommunications Union, [ITU-R, 1997](#)). IRI is used to compute monthly median values of  $f_0F2$  and  $M_{3000}F2$  for any given latitude, longitude, month, universal time, and solar activity, and the obtained values are converted to  $N_mF2$  and  $h_mF2$  using the following relations ([Bilitza et al., 1979](#)):

$$N_mF2 = 1.24 \times 10^{10} \cdot f_0F2^2, \quad (1)$$

where  $f_0F2$  is measured in MHz and  $N_mF2$  in  $\text{elec}/\text{m}^{-3}$ ; and:

$$h_mF2 = \frac{1490}{M_{3000}F2 + CF} - 176, \quad (2)$$

where  $h_mF2$  is measured in km and the correction factor is given by:

$$CF = \frac{[0.00232 \cdot R_{12} + 0.222] \cdot \left[1 - \frac{R_{12}}{150} \exp\left(-\frac{\vartheta^2}{1600}\right)\right]}{\frac{f_0F2}{f_0E} - 1.2 + 0.0116 \cdot \exp(0.0239 \cdot R_{12})} + 0.00064 \cdot (R_{12} - 25), \quad (3)$$

in which  $\vartheta$  is the geomagnetic latitude,  $R_{12}$  is the 12-month running mean value of the monthly mean sunspot number, and  $f_0E$  is the  $E$ -layer critical frequency, which is computed as function of the solar zenith angle, the geographic latitude and the solar activity, according to the [ITU-R \(1997\)](#) recommendations.

Since 2006, the C/F-3 mission team has delivered ROP to the scientific community through the Data Analysis and Archival Center (CDAAC) database at the University Corporation for Atmospheric Research (UCAR; <http://cdaac-www.cosmic.ucar.edu/>). At monthly intervals, these ROP sample the global ionosphere quite homogeneously in space and time, providing new opportunities for developing the science and the technology associated to the ionosphere. As any new tool, ROP must face the distrust of researchers before being accepted (or discarded), but much work has been (and is being) done to assess the real accuracy of the parameters derived from ROP. Most papers (e.g.: [Jakowski et al., 2004](#); [Schreiner et al., 2007](#); [Angling, 2008](#); [Yue et al., 2010](#); [Zhang et al., 2010](#); [Krakowski et al., 2011](#)) reported good agreement with ionosondes at mid latitude and some degradation at low latitudes, especially in the equatorial anomaly region. Without trying to establish conclusive values for such errors, the above mentioned studies allow us to set the RMS of the differences between ROP and ionosonde to be around 8% for  $N_mF2$  and 5% for  $h_mF2$ .

In order to automatically scan the CDAAC database and mitigate the impact of unreliable ROP in the results of this research we applied a processing strategy based on fitting every ROP with the La Plata Ionospheric Model (LPIM; [Brunini et al., 2013](#)), and carefully checking the statistical significance of the differences between the ROP and LPIM. This procedure does not guarantee the

accuracy of the retrieved parameters, but performs reasonably well in filtering out automatically many unreliable observations and also unreliable ROP (a task that cannot be done manually due to the huge amount of data). By ‘reasonably’ we understand that most of the filtered data are indisputably unreliable, that most of the accepted data cannot be rejected with the available information, and that the filtering criterion do not bias the data in favor of any local time or modip. In addition, this procedure reasonably assesses the precision of the estimated parameters (at least, as reasonably as the Least Squares theory allows); but it cannot assess the accuracy of the estimated parameters. For that reason, we tried to isolate the day-to-day variability from the IRI–ROP differences, and further, we do not focus on the interpretation of these systematic differences. Indeed, we called such systematic differences the ‘combined IRI–ROP bias’, just to highlight the fact that both sources (IRI and ROP) would be contributing to such systematic. We have focused on the day-to-day variability, and for its computation we subtracted the standard deviation of the estimated parameters (provided by the Least Square method) from the standard deviation of the IRI–ROP differences, as it is explained in the next Section.

## 2. Retrieving $N_mF2$ and $h_mF2$ from radio-occultation profiles

The LPIM model uses four  $\alpha$ -Chapman layers to represent the electron density as a function of the height in the  $E$  and  $F1$  layers and in the bottom- and top-side of the  $F2$  layer. The entire LPIM profile is anchored to three parameters:  $N_mF2$ ,  $h_mF2$  and  $HF2$  (the scale height) of the  $F2$  layer. Once the values of these parameters are given, LPIM computes all the other parameters involved in the bottom-side formulation according to the [ITU-R \(1997\)](#) recommendations. The parameters involved in the top-side formulation (the transition height where the dominant ion species changes from  $O^+$  to  $H^+$ ; the scale height at the transition height; and the shape parameter of the topside profile) are evaluated according to [Meza et al. \(2008\)](#).

In summary, for any given latitude, longitude, height and universal time, the LPIM electron density is given by a function that depends on the three parameters  $N_mF2$ ,  $h_mF2$  and  $HF2$ , whose values are estimated by fitting the LPIM to every single ROP, using a re-weighted Least Squares procedure. The weights of all electron density values in a given ROP are initially set to 1, and are iteratively modified according to the ‘bisquare’ criterion ([Huber, 1981](#)). The iteration is stopped when the changes in the estimated parameters became negligible. We tuned the processing algorithm so as to reject indisputably wrong data, and to accept indisputably correct ones. In addition, we checked that the data in the ‘gray zone’ (either accepted or discarded) did not exert great influence on the final results. The application of this procedure led us to assign negligible weights (which in practice is equivalent to discarding the data) to  $\sim 20\%$  of the available data (including complete ROP). Approximately 50% of the discarded data

was indisputably wrong. In the other half of cases, it was difficult to determine whether the misalignment between ROP and LPIM should be attributed to problems on the data, the model, or both.

As is known, the Least Squares method provides estimates of the errors of the estimated parameters. This error estimation is related to the precision, but not to the accuracy of the estimated parameters, i.e.: the error estimation reports on the agreement between the data and the fitted model, but not on the presence of systematic errors in the data nor in the model. The errors estimated in this study for  $N_mF2$  and  $h_mF2$  (more explicitly, the standard deviation of  $N_mF2$  and  $h_mF2$ ) ranged around 1% of the values of the estimated parameters.

### 3. Establishing the statistical model

Let  $\Omega_{\text{ROP}}$  be either the  $N_mF2$  or  $h_mF2$  parameter retrieved from a given ROP, and  $\hat{\sigma}_{\text{ROP}}$  the corresponding standard deviation estimated with the Least Squares procedure described in the previous section; and let  $\Omega_{\text{IRI}}$  be the monthly median value of the corresponding parameter computed with IRI according to the procedure explained in Section 1. The statistical model we are going to propose is based on the difference between the IRI and the ROP parameters:

$$\Delta = \Omega_{\text{IRI}} - \Omega_{\text{ROP}}, \quad (4)$$

and on the following hypotheses:

1. the IRI parameters are affected by errors that are statistically distributed with  $b_{\text{IRI}}$  mean (attributed to a systematic bias in the monthly median parameters computed by IRI) and  $\sigma_{\text{IRI}}$  standard deviation (attributed to the day-to-day variability of the parameters that is averaged in their monthly median values); and
2. the ROP parameters are affected by errors that are statistically distributed with  $b_{\text{ROP}}$  mean and  $\sigma_{\text{ROP}}$  standard deviation (attributed to errors in the data and models used to derive the ROP from the raw measurements and to estimate the parameters from the ROP).

After Eq. (4) and hypotheses (1) and (2) it follows that:

$$b_{\Delta} = b_{\text{IRI}} - b_{\text{ROP}}, \quad \text{and} \quad (5)$$

$$\sigma_{\Delta}^2 = \sigma_{\text{IRI}}^2 + \sigma_{\text{ROP}}^2, \quad (6)$$

where  $b_{\Delta}$  and  $\sigma_{\Delta}$  are the IRI–ROP combined bias and standard deviation.

In addition, we assume that the combined IRI–ROP bias,  $b_{\Delta}$ , and the day-to-day standard deviation of IRI,  $\sigma_{\text{IRI}}$ , behave as functions that primarily depend on five variables: month, local time, solar activity measured by  $IG_{12}$  index, geomagnetic activity measured by the  $A_p$  index, and modip latitude. Under this assumption, we can get an empirical estimation of the combined IRI–ROP bias and the day-to-day standard deviation of IRI, by sorting the  $\Delta$  differences in the following five dimensional grid:

1. month: from 1 to 12 in intervals of 1 month;
2. local time: from  $-1$  to 23 in intervals of 2 h;
3. solar activity: only low solar activity conditions are considered, given by  $IG_{12} < 20$ ;
4. geomagnetic activity: only quiet geomagnetic days are considered, given by  $A_p < 15$ ;
5. modip: from  $-60$  to  $+60$  in intervals of 10 degrees.

If  $\Delta_i$  and  $\hat{\sigma}_{\text{ROP},i}$ ,  $i = 1, \dots, n$ , are the differences and the standard deviations computed from the  $n$  ROP contained within a given bin of the five-dimensional grid, we can estimate the combined IRI–ROP bias and the day-to-day standard deviation of IRI for the corresponding node as:

$$\hat{b}_{\Delta} = \frac{1}{n} \sum_{i=1}^n \Delta_i, \quad \text{and} \quad (7)$$

$$\hat{\sigma}_{\text{IRI}} = \sqrt{\hat{\sigma}_{\Delta}^2 - \hat{\sigma}_{\text{ROP}}^2}, \quad \text{where} \quad \hat{\sigma}_{\Delta}^2 = \frac{1}{n-1} \left[ \sum_{i=1}^n (\Delta_i - \hat{b}_{\Delta})^2 \right],$$

$$\text{and} \quad \hat{\sigma}_{\text{ROP}} = \frac{1}{n} \sum_{i=1}^n \hat{\sigma}_{\text{ROP},i}^2. \quad (8)$$

### 4. Results and discussion

We used ROP downloaded from the CDAAC database comprised within the period January 1, 2007–October 10, 2010. Within this period, the solar activity remained low, with the  $IG_{12}$  index varying from approximately 7 (at the beginning) to 20 (at the end), and reaching a minimum of  $-10$  on August 2011. We retained only quiet geomagnetic days with  $A_p$  index lower than 15. We note that [Cander and Haralambous \(2011\)](#) have shown that these conditions do not guarantee a smooth behavior of ionosphere parameters: analyzing vertical Total Electron Content (TEC) derived from Global Navigation Satellite Systems (GNSS) receivers over the European sector, they found 24 sudden increases of TEC events, all occurred during the period 2008–2009 and under very weak geomagnetic disturbances. We have not traced these events, so they are present in our dataset and contribute to the day-to-day standard deviation of IRI that will be discussed in the next paragraphs.

Considering all months, local times, and modip under low solar and geomagnetic activity, we analyzed a dataset of more than  $2.5 \times 10^4$  ROP (validated with the procedure described in Section 2), distributed in almost 1300 low solar activity and quiet geomagnetic days (i.e.: approximately 6000 ROP per month). we found a combined IRI–ROP bias of  $+17.3\%$  for  $N_mF2$  and of  $+0.5\%$  for  $h_mF2$ . The analyzed period includes the extremely low solar minimum between solar cycles 23 and 24, for which [Solomon et al. \(2013\)](#) reported a  $N_mF2$  global mean  $\sim 15\%$  lower than for the preceding minimum. Furthermore, [Araujo-Pradere et al. \(2013\)](#) reported that the  $h_mF2$  values predicted by IRI agreed quite well with the measurements during the 22/23 solar minimum, but overestimated the measurements during the 23/24 solar minimum. These

results would support the conjecture that IRI tends to overestimate the parameters of the F2 peak, especially  $N_mF2$ , when the intensity of the extreme ultraviolet radiation from the sun decreases to as low as the values recorded during the 2008–2009 solar minimum. However, we want to be cautious when interpreting the combined IRI–ROP bias until having an accurate evaluation of the systematic errors that might arise from the ROP.

As pointed out in Section 1, we used the Bilitza formula (Eqs. (2) and (3)) to convert the  $M_{3000}F2$  propagation factor to the  $h_mF2$  height. Searching for evidences of long-term cooling of the upper atmosphere, Ulich and Turunen (1997) analyzed a long time series of ionosonde data recorded at the Finland station Sodankylä (67.4°N, 26.7°E). In that research they attributed to the Bilitza formula an overestimation of 18 km (on average) in the prediction of the  $h_mF2$  height. We have compared the  $h_mF2$  heights obtained by conversion with the Bilitza formula of the  $M_{3000}F2$  values provided by IRI, to the  $h_mF2$  heights derived from the ROP. We tried to reproduce the conditions of the Ulich and Turunen study, so we extracted from our dataset the observations comprised within a modip range of 5° wide centered on the modip latitude of the Sodankylä station, and within the 10–14 local time interval. The results are displayed in the Fig. 1: the upper panel shows the  $h_mF2$  heights derived from IRI using the Bilitza formula (red dots), and the corresponding heights derived from the ROP (blue dots); the lower panel shows the differences in the sense IRI–ROP. The horizontal dashed line is the mean value of these differences, which were  $+10.4 \pm 14.9$  km. Although this value is not far from the one determined by Ulich and Turunen, we do not feel confident to speculate on the existence of a systematic bias in the Bilitza formula.

Figs. 2–5 represent the combined IRI–ROP bias and the day-to-day standard deviation of IRI. They present the

results for  $N_mF2$  and  $h_mF2$ , for two selected local time intervals: one centered at noontime ( $11 \leq LT < 13$ ) and the other centered at midnight ( $23 \leq LT < 01$ ). The month is given along the  $x$ -axis and the modip along the  $y$ -axis. Both the combined IRI–ROP bias and the day-to-day standard deviation of IRI are given in percent of the monthly median value of the corresponding parameter computed with IRI. Graphical representations of these monthly median values are also provided in order to help in interpreting the results (in units of  $10^{10}$  elec/m<sup>3</sup> for  $N_mF2$  and km for  $h_mF2$ ).

Regarding  $N_mF2$ , it can be stated that:

1. there is a systematic bias between IRI and ROP, that at noon time reaches 35% over the crests of the Equatorial Anomaly; and at midnight reaches 50% for almost all seasons and modip; and
2. the day-to-day variation of IRI is characterized by a standard deviation that, at noontime, varies from  $\pm 10\%$  to  $\pm 30\%$ , with maxima over the northern and southern crests of the Equatorial Anomaly; and, at midnight, varies from  $\pm 20\%$  to  $\pm 45\%$ , with the greatest values occurring in the equatorial region during the months of May and September.

Regarding  $h_mF2$ , it can be stated that:

1. there is a systematic bias between IRI and ROP, that at noontime ranges from  $-4\%$  to  $+12\%$  (IRI greater than ROP in the equatorial and mid latitude regions, and lower than ROP over the crests of the Equatorial Anomaly); and at midnight ranges from  $-8\%$  to  $+2\%$  (IRI generally lower than ROP, except in the limit between the mid and high latitude regions); and
2. the day-to-day variation of IRI is characterized by a standard deviation that, at noontime varies from  $\pm 2\%$  to  $\pm 10\%$  with minima over the modip equator; and, at

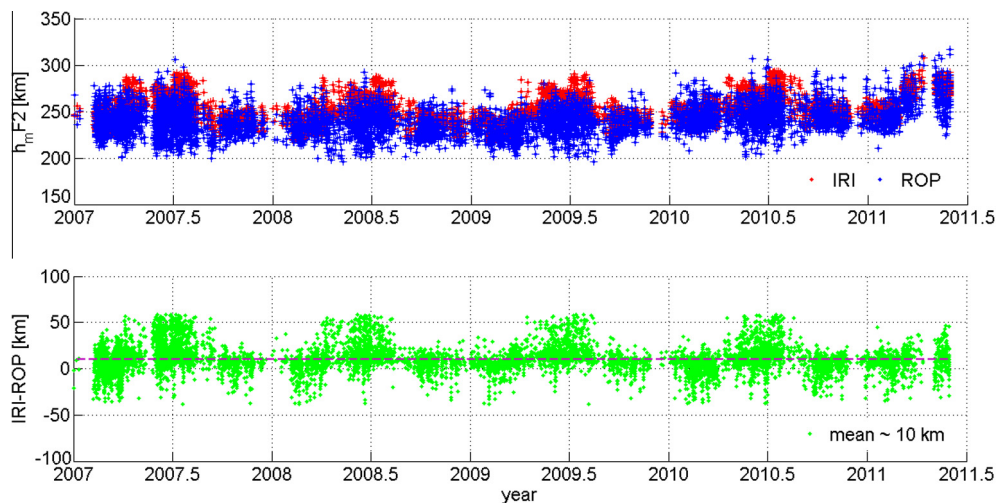


Fig. 1.  $h_mF2$  heights derived from IRI using the Bilitza formula (upper panel red dots), and the corresponding heights derived from the ROP (upper panel blue dots); and differences in the sense IRI–ROP (lower panel), including the mean value of these differences (dashed line). (For interpretation of the references to colour in this figure legend, the reader is referred to the web version of this article.)



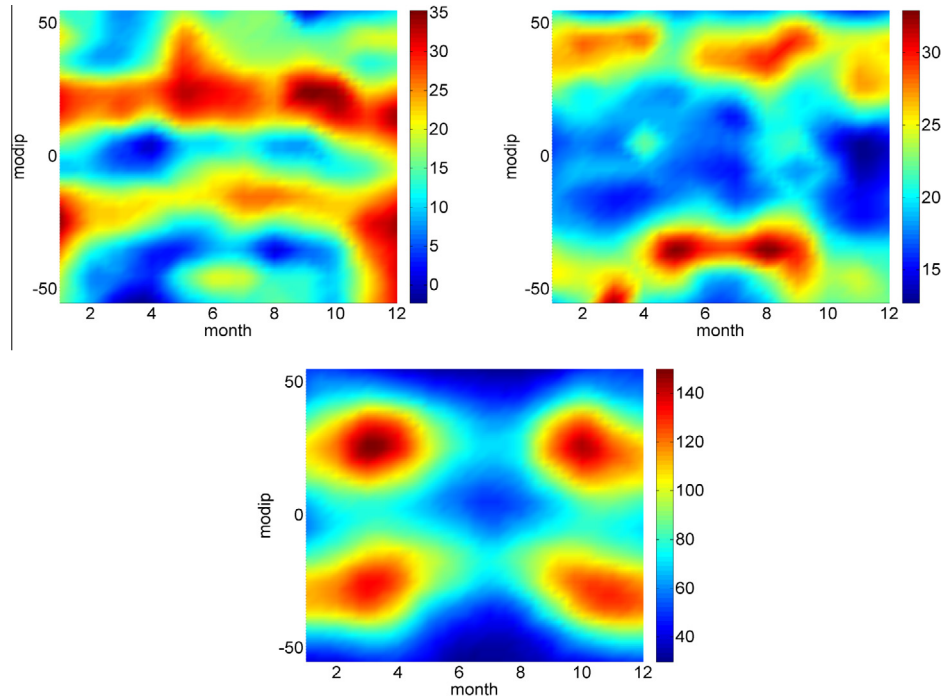


Fig. 2. Noontime IRI–ROP bias (upper left) and standard deviation of the day-to-day variability (upper right), in percents of the monthly median value of  $N_mF2$ , which is represented in the bottom panel in units of  $10^{10}$  elec/m<sup>3</sup>.

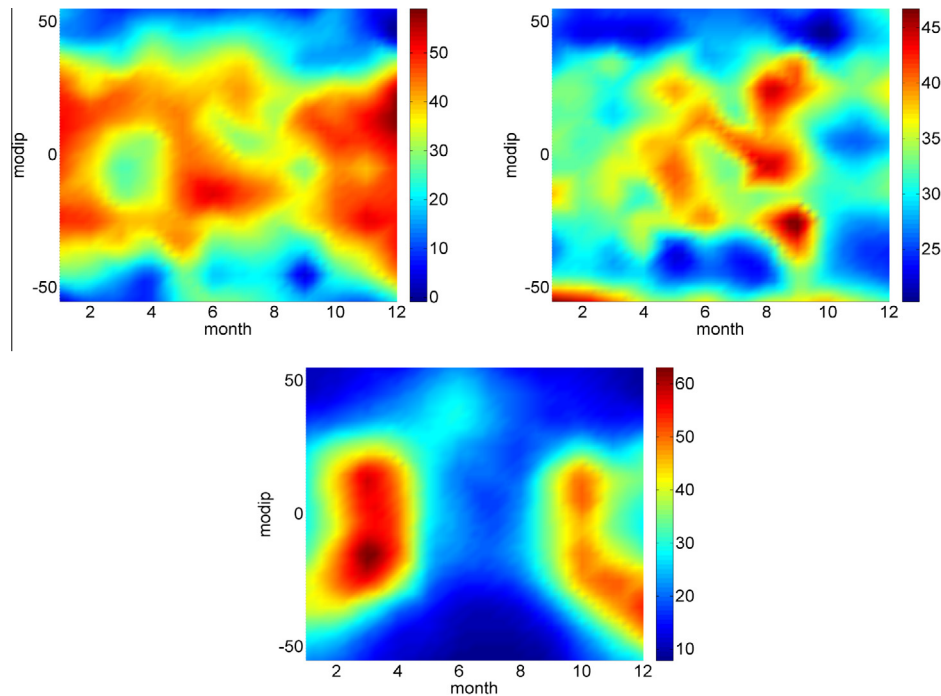


Fig. 3. Midnight IRI–ROP bias (upper left) and standard deviation of the day-to-day variability (upper right), in percents of the monthly median value of  $N_mF2$ , which is represented in the bottom panel in units of  $10^{10}$  elec/m<sup>3</sup>.

midnight varies from  $\pm 3\%$  to  $\pm 11\%$ , with the greatest values in the equatorial region from January to May and from September to January.

The problem of establishing a statistical model for the ionosphere variability has been faced, among others, by

Wilkinson (1995, 2004). In the latter paper he conducts an exhaustive study involving 9 ionosonde stations in Australia, and in accordance to the ITU-R recommended procedure (ITU-R, 1997), he describes the day-to-day variability of the  $f_0F2$  parameter in terms of the upper and lower deciles of the observed distribution. More

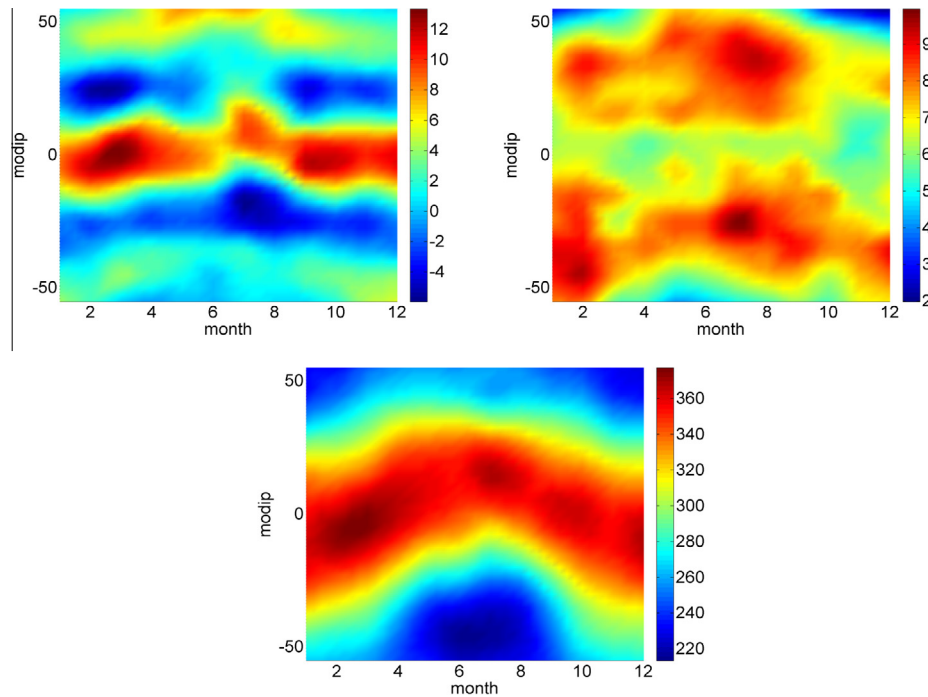


Fig. 4. Noontime IRI–ROP bias (upper left) and standard deviation of the day-to-day variability (upper right), in percents of the monthly median value of  $h_mF2$ , which is represented in the bottom panel in km.

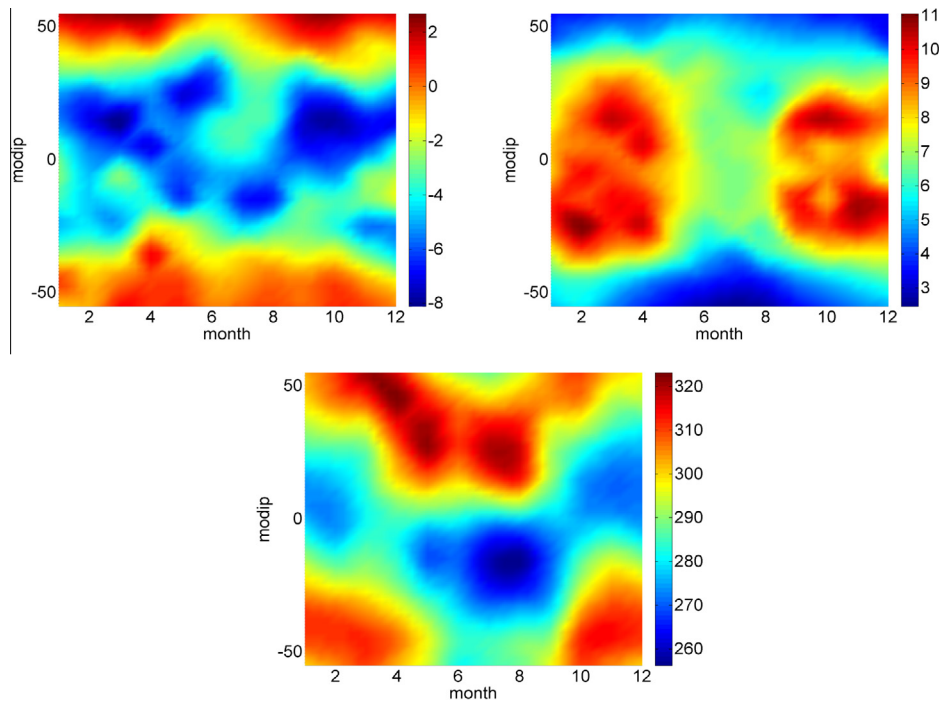


Fig. 5. Midnight IRI–ROP bias (upper left) and standard deviation of the day-to-day variability (upper right), in percents of the monthly median value of  $h_mF2$ , which is represented in the bottom panel in km.

specifically, he uses the decile factors defined as the ratio between the upper or lower decile and the monthly median value computed with the IRI. In order to compare our results to the ones reported by Wilkinson, we extracted from our dataset the observations comprised within a modip range of  $5^\circ$  wide centered on the modip latitude of

the Canberra station ( $35.3^\circ\text{S}$ ,  $149.0^\circ\text{E}$ ), and within the 23.5–00.5 local time interval. In spite of this, the results are not directly comparable because the Wilkinson study comprised a high solar activity periods, with  $R_{12} > 100$ , while our study comprises a low solar activity period with  $R_{12} < 50$ . Fig. 6 displays the monthly variation of the lower

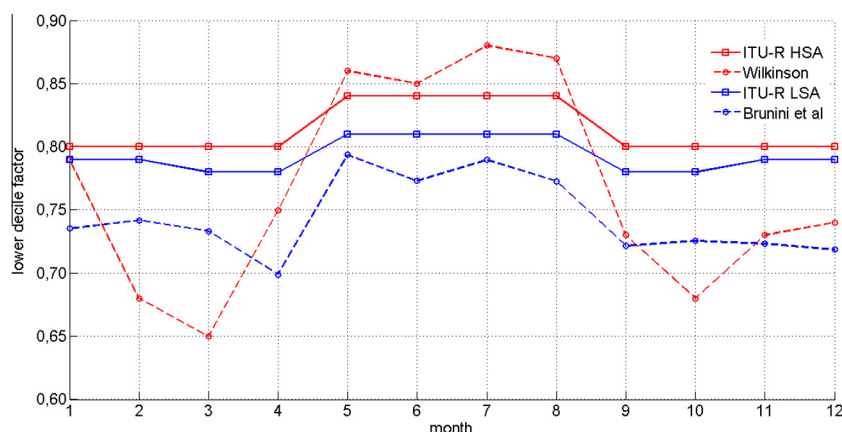


Fig. 6. Monthly variation of the lower decile factor for  $f_0F_2$  according to: (a) ITU-R for high solar activity (red solid line); (b) Wilkinson (2004) for high solar activity (red dashed line); (c) ITU-R for low solar activity (solid blue line); and (d) this study for low solar activity (dashed blue line). (For interpretation of the references to colour in this figure legend, the reader is referred to the web version of this article.)

decile factor for  $f_0F_2$  according to: (a) ITU-R for high solar activity (red solid line); (b) Wilkinson for high solar activity (red dashed line); (c) ITU-R for low solar activity (solid blue line); and (d) this study for low solar activity (dashed blue line). According to our view, neither of the two studies differ significantly from the variability model proposed by ITU-R: the study by Wilkinson shows that when solar activity is high, the observed variability is slightly lower (1–5%) in the winter months, and higher (1–19%) in the summer and equinoctial months; while our study shows that when solar activity is low, the observed variability is always a slightly higher (2–9%).

## 5. Summary and conclusion

This work is intended to be a contribution toward the development of a statistical model to assess the expected deviation of the monthly median values of  $N_mF_2$  and  $h_mF_2$  computed by IRI with respect to their actual values, which were retrieved from C/F-3 ROP. The differences between the IRI and ROP parameters were interpreted as the summation of systematic biases and random errors in both IRI and ROP. The systematic and random components were empirically separated, and the random component attributed to IRI was empirically isolated from the random component attributed to ROP. The standard deviation of the random component attributed to IRI was interpreted to be representative of the day-to-day variability of the ionospheric parameters that is averaged in the monthly median values computed by IRI. This day-to-day variability was analyzed as a function that primarily depends on the month, solar activity, geomagnetic perturbation, local time and modip. For the low solar activity and quiet geomagnetic days analyzed in this research, the standard deviation of the day-to-day variability was found to vary according to (percent of the monthly median value computed with IRI):

- $N_mF_2$  at noontime:  $\pm 10\%$  to  $\pm 30\%$  with maxima over the northern and southern crests of the Equatorial Anomaly;
- $N_mF_2$  at midnight:  $\pm 20\%$  to  $\pm 45\%$ , with the greatest values in the equatorial region during the months of May and September;
- $h_mF_2$  at noontime:  $\pm 2\%$  to  $\pm 10\%$  with minima over the modip equator;
- $h_mF_2$  at midnight:  $\pm 3\%$  to  $\pm 11\%$  with the greatest values in the equatorial region from January to May and from September to January.

Regarding the systematic difference between the IRI and ROP parameters, it seems reasonable to conjecture that systematic errors on both sides contribute to them. From the side of IRI, some responsibility could be attributed to limitations of the Jones and Gallet's mapping technique, as well as to limitations in the dataset used to establish the ITU-R coefficients. In the case of ROP, systematic errors may arise from difficulties of the radio occultation technique to cope with steep horizontal gradients in the electron content distribution. The analysis performed in this work does not allow us to determine which part of the systematic error (which in the case of  $N_mF_2$  reaches 50%) must be attributed to each of the sources.

## References

- Angling, M.J., 2008. First assimilations of COSMIC radio occultation data into the electron density assimilative model (EDAM). *Ann. Geophys.* 26, 353–359. <http://dx.doi.org/10.5194/angeo-26-353-2008>.
- Anthes, R.A., Bernhardt, P.A., Chen, Y., Cucurul, L., Dymond, K.F., Ector, D., Healy, S.B., Ho, S.-P., Hunt, D.C., Kuo, Y.-H., Liu, H., Manning, K., McCormick, C., Meehan, T.K., Randel, W.J., Rocken, C., Schreiner, W.S., Sokolovskiy, S.V., Syndergaard, S., Thompson, D., Trenberth, K.E., Wee, T.-K., Yen, N.L., Zeng, Z., 2008. The COSMIC/FORMOSAT 3 mission – early results. *Bull. Am. Meteorol. Soc.* 313–333, 2008.
- Araujo-Pradere, E.A., Buresova, D., Fuller-Rowell, D.J., Fuller-Rowell, T.J., 2013. Initial results of the evaluation of IRI hmF2 performance

- for minima 22–23 and 23–24. *Adv. Space Res.* 51 (4), 630–638. <http://dx.doi.org/10.1016/j.asr.2012.02.010>.
- Bilitza, D., McKinnell, L.-A., Reinisch, B., Fuller-Rowell, T., 2011. The international reference ionosphere (IRI) today and in the future. *J. Geod.* 85, 909–920. <http://dx.doi.org/10.1007/s00190-010-0427-x>.
- Bilitza, D., Sheikh, N.M., Eyfrig, R., 1979. A global model for the height of the F2-peak using M3000 values from the CCIR numerical map. *Telecommun. J.* 46, 549–553.
- Brunini, C., Azpilicueta, F., Nava, B., 2013. A technique for routinely updating the ITU-R database using radio occultation electron density profiles. *J. Geod.* 87 (9), 813–823. <http://dx.doi.org/10.1007/s00190-013-0648-x>.
- Cander, L.R., Haralambous, H., 2011. On the importance of the total electron content enhancements during the extreme solar minimum. *Adv. Space Res.* 47 (2), 304–311. <http://dx.doi.org/10.1016/j.asr.2010.08.026>.
- Huber, P.J., 1981. *Robust Statistics*. John Wiley and Sons, New York.
- ITU-R Recommendation ITU-R P.1239, ITU-R reference ionospheric characteristics, International Telecommunications Union, Radio Communication Sector, Geneva, 1997.
- Jakowski, N., Leitinger, R., Angling, M., 2004. Radio occultation techniques for probing the ionosphere. *Ann. Geophys.* 47, 1049–1066.
- Jones, W.B., Gallet, R.M., 1962. Representation of diurnal and geographical variations of ionospheric data by numerical methods. *ITU Telecommun. J.* 29 (5), 129–149.
- Jones, W.B., Gallet, R.M., 1965. Representation of diurnal and geographical variations of ionospheric data by numerical methods – control of stability. *ITU Telecommun. J.* 32 (1), 18–28.
- Jones, W.B., Obitts, D.L., 1970. Global representation of annual and solar cycle variations of foF2 monthly median 1954–1958, Telecomm. Research Report, OT/ITS/RR3, Washington DC, USA, US Government Printing Office.
- Krankowski, A., Zakharenkova, I., Krypiak-Gregorczyk, A., Shagimuratov, I.I., Wielgosz, P., 2011. Ionospheric electron density observed by FORMOSAT-3/COSMIC over the European region and validated by ionosonde data. *J. Geod.* 85, 949–964. <http://dx.doi.org/10.1007/s00190-011-0481-z>.
- Meza, A., Gualarte Scarone, E., Brunini, C., Mosert, M., 2008. Analysis of a topside ionospheric model using GPS and ionosonde observables. *Adv. Space Res.* 42, 712–719. <http://dx.doi.org/10.1016/j.asr.2007.08.042>.
- Schreiner, W., Rocken, C., Sokolovskiy, S., Syndergaard, S., Hunt, D., 2007. Estimates of the precision of GPS radio occultations from the COSMIC/FORMOSAT-3 mission. *Geophys. Res. Lett.* 34, L04808. <http://dx.doi.org/10.1029/2006GL027557>.
- Solomon, S.C., Qian, L., Burns, A.G., 2013. The anomalous ionosphere between solar cycles 23 and 24. *J. Geophys. Res. Space Phys.* 118 (10), 6524–6535. <http://dx.doi.org/10.102/jgra.50561>.
- Ulich, T., Turunen, E., 1997. Evidence for long-term cooling of the upper atmosphere in ionosonde data. *Geophys. Res. Lett.* 24, 1103–1106.
- Wilkinson, P.J., 2004. Ionospheric variability and the international reference ionosphere. *Adv. Space Res.* 34, 1853–1859. <http://dx.doi.org/10.1016/j.asr.2004.08.007>.
- Wilkinson, P.J., 1995. Predictability of ionospheric variations for quiet and disturbed conditions. *J. Atmos. Terr. Phys.* 57, 1469–1481.
- Yue, X., Schreiner, W.S., Lei, J., Sokolovskiy, S.V., Rocken, C., Hunt, D.C., Kuo, Y.-H., 2010. Error analysis of Abel retrieved electron density profiles from radio occultation measurements. *Ann. Geophys.* 28, 217–222. <http://dx.doi.org/10.5194/angeo-28-217-2010>.
- Zhang, M.-L., Liu, C., Wan, W., Liu, L., Ning, B., 2010. Evaluation of global modeling of M(3000)F2 and hmF2 based on alternative empirical orthogonal function expansions. *Adv. Space Res.* 46, 1024–1031. <http://dx.doi.org/10.1016/j.asr.2010.06.004>.